Phosphatidylethanolamine is a phagocytic ligand implicated in the binding and removal of microbial extracellular vesicles

Ava Kavianpour[1,2], Kirsten J. Meyer[2], Trieu Le[1], Pedro Elias Marques[3], Justin R. Nodwell[2], Spencer A. Freeman[1,2*]

[1]Program in Cell Biology, Peter Gilgan Centre for Research and Learning, Hospital for Sick Children, 686 Bay Street, 19-9800, Toronto, ON, M5G 0A4, Canada.

[2]Department of Biochemistry, Temerty Faculty of Medicine, University of Toronto, Toronto, Ontario, Canada.

[3]Laboratory of Molecular Immunology, Department of Microbiology, Immunology and Transplantation, Rega Institute for Medical Research, KU Leuven, 3000, Leuven, Belgium

*Correspondence to: Spencer Freeman (spencer.freeman@sickkids.ca)

Keywords: phagocytosis, macrophage, CD300, Syk, integrins, phosphatidylethanolamine (PE), phosphatidylserine (PS), extracellular vesicles

Abstract

The efficient recognition and removal of apoptotic cells by phagocytes is critical to prevent secondary necrosis and maintain tissue homeostasis. Such detection involves receptors and bridging molecules that recognize lipids –normally restricted to the inner leaflet of healthy cells– which become exposed on the surface of dead cells and the vesicles they produce. A majority of studies focus on phosphatidylserine (PS) for which there are well-established receptors that either bind to the lipid directly or indirectly via intermediary proteins. Phosphatidylethanolamine (PE) is even more prevalent than PS in the inner leaflet of mammalian cells and also becomes exposed by the action of scramblases during cell death, though little is known about the effects of PE once scrambled. Here, we report that PE can itself serve as a phagocytic ligand for macrophages by engaging CD300 family receptors. CD300a and CD300b specifically modulated PE-mediated uptake, and this process involved integrins and spleen tyrosine kinase (Syk). For bacteria, which contain PE but largely lack PS in their membranes, we report that PE engagement enabled the binding and uptake of spheroplasts and extracellular vesicles (EVs) that were unsheathed by the cell wall. Based on these observations, we posit that the direct recognition of PE facilitates mechanisms of clearance that stand to have a broad impact on the immune response.

Introduction

The lipid bilayers that separate cells from their external environment are made asymmetric in their distribution of lipids by resident lipid-binding proteins (Doktorova *et al*, 2020; Lorent *et al*, 2020; Sakuragi & Nagata, 2023; Verkleij *et al*, 1973). Energy-dependent flippases ensure that lipids like PS and PE remain tightly restricted in their incorporation to the cytoplasmic (inner) leaflet while floppases generate enrichment of phosphatidylcholine (PC) and sphingolipids in the exofacial (outer) leaflet (Bretscher, 1972; Lorent *et al.*, 2020; Verkleij *et al.*, 1973). This is a highly conserved process: though the lipid species concentrations vary in the membrane bilayer between eukaryotes and prokaryotes, the asymmetric nature of plasma membranes is universal (Bogdanov *et al*, 2020; Sohlenkamp & Geiger, 2016). Upon cell death, lipid scramblases of the bilayer become active such that asymmetry is lost (Sakuragi & Nagata, 2023). The exposure of lipids normally restrained to the inner leaflet is the major determinant for the removal of the cell by phagocytosis. This has largely been described for PS which has well-established receptors (Doran *et al*, 2020; Lemke, 2019; Segawa & Nagata, 2015).

Despite widespread emphasis on PS in initiating the phagocytic programs that remove dead cells, PE is just as prevalent and equally restricted to the inner leaflet of healthy mammalian cells (Lorent *et al.*, 2020). In healthy cells, like PS, PE is only translocated to the outer leaflet during specific cellular events including at the cleavage furrow when cells divide (Emoto *et al*, 1996), and to initiate cell-cell fusion that supports the formation of multinucleated osteoclasts (Irie *et al*, 2017). Otherwise, PE is only reported to be scrambled during cell death (Emoto *et al*, 1997; Zhao *et al*, 2008). While the individual scramblase(s) responsible for exposing PE are not entirely elucidated, the original discovery of the Ca^{2+}-activated TMEM16F as a lipid scramblase demonstrated its capacity to scramble PE (Suzuki *et al*, 2010). The Xkr8 scramblase of the XKR

family can also scramble PS and PE in cells undergoing apoptosis (Suzuki *et al*, 2013). It is noteworthy that in prokaryotes, PE in fact predominates over PS, which is of low abundance (Doktorova *et al.*, 2020). While the lipid membrane of bacteria is masked by surface sugars making up the cell wall, bacteria are known to secrete extracellular vesicles (EVs) devoid of cell wall components (Briaud & Carroll, 2020; Brown *et al*, 2015; Toyofuku *et al*, 2023) and their cell wall can also be removed by lysozyme to expose the outer membrane (Ragland & Criss, 2017). How host immune cells recognize bacterial debris or EVs is poorly understood.

In that regard, the highly expressed CD300 family of immunoreceptors present in phagocytic cells are known to recognize both PS and PE (Cannon *et al*, 2012; Murakami *et al*, 2014; Nakahashi-Oda *et al*, 2012; Simhadri *et al*, 2012; Yamanishi *et al*, 2010). Here we report that the relative engagement of CD300a, an inhibitory receptor, and CD300b, an activating receptor dictates the outcome of PE-mediated phagocytosis. PE particles were found to be engaged and phagocytosed by primary macrophages to an equal extent as PS particles. Moreover, PE-receptors function in the binding and uptake of bacterially-derived spheroplasts and extracellular vesicles. Thus, we posit PE as a critical mediator of host-pathogen intracellular communication and an underappreciated phagocytic ligand.

Results

Lipid scrambling by the Ca^{2+}-activated scramblase TMEM16F exposes exofacial PE

Scrambling of the plasma membrane bilayer is common to all types of cell death. To investigate PS and PE, lipids that are normally kept harbored in the inner leaflet by the activity of flippases (**Fig 1A**), we generated and applied established lipid probes. To this end, PS can be visualized using recombinant Lactadherin C2 fused to GFP (LactC2-GFP) (Kay & Grinstein,

2011) while PE can be visualized using Duramycin-iFluor555 (Dura-555) (Zhao *et al.*, 2008). To validate the specificity of the probes, lipid-coated beads containing either 5% PS or PE and 95% phosphatidylcholine (PC) were incubated with both probes simultaneously and imaged using fluorescence confocal microscopy. Importantly, LactC2-GFP only labelled the lipid-coated beads that contained PS while Dura-555 only labelled those containing PE (**Fig 1B**).

TMEM16F, a Ca^{2+}-activated lipid scramblase, is reported to be essential for the scrambling of PS in response to sustained, elevated concentrations of Ca^{2+} in the cytosol in various cell types (Suzuki *et al.*, 2010). While TMEM16F can scramble a diverse array of lipids including PS, PE, and phosphatidic acid among others, the role of TMEM16F in scrambling PE during programmed cell death has not been established. We first treated RAW264.7 cells acutely (15 min) with the Ca^{2+} ionophore, ionomycin, to increase cytosolic [Ca^{2+}] and the stimulation of Ca^{2+}-activated scramblases. This treatment led to membrane blebbing and the robust exposure of PS and PE on the exofacial leaflet of the membrane bilayer as judged by the accumulation of LactC2-GFP and Dura-555 on the surface of the cells (**Fig 1C**). Similar results were obtained when treating cells with staurosporine (STS) for longer periods (3 h) which leads to apoptosis (**Fig 1C**). This contrasted with RAW264.7 cells in which TMEM16F was ablated: TMEM16F KO cells treated with ionomycin did not expose PS or PE and did not undergo membrane blebbing (**Fig 1C**) as previously reported by others in non-macrophage cell types upon Ca^{2+} influx (Han *et al*, 2019; Wu *et al*, 2020).

Importantly, increasing cytosolic Ca^{2+} with ionophores has effects on the plasma membrane beyond lipid scrambling. It also leads to the activation of phospholipases which hydrolyze $PI(4,5)P_2$, causing delamination of the cytoskeleton from the membrane, and to the activation of many other pathways that grossly change cell morphology. To determine if the

activation of TMEM16F, independent of elevating Ca^{2+}, is sufficient to cause scrambling of PE, we generated cell lines that can be induced with doxycycline to express WT TMEM16F- or TMEM16F Y563Q-GFP, a form of the scramblase that is made constitutively active even without increased cytosolic Ca^{2+} (Le *et al*, 2019). Upon treating the cells with doxycycline, TMEM16F-GFP was synthesized and localized to the secretory pathway and, prominently, to the surface membrane (**Fig 1D**). Convincingly, the expression of the active but not WT form of the scramblase let to the scrambling and exposure of both PS and PE and, curiously, caused vesiculation of the cells (**Fig 1D**). This suggests that TMEM16F activation alone leads to the exposure of PE together with PS.

PE is a phagocytic ligand

While PS is a well-appreciated phagocytic ligand, PE has not been investigated in the context of phagocytosis. To first investigate if PE could in principle serve as a phagocytic ligand, RAW264.7 cells were incubated with beads coated with PC together with either 5% PS or PE for 10 min in serum free medium. Both PS- and PE-containing lipid coated beads were bound by the RAW264.7 cells, while beads coated with PC alone were not (**Fig 2A-B**). Interestingly, the lipid-coated beads appeared tethered to the surface of the RAW264.7 cells but not obviously internalized (**Fig 2A**). RAW264.7 cells are poorly efferocytic when compared to primary macrophages. Therefore, to investigate if PE could serve as a *bona fide* phagocytic ligand, bone marrow-derived macrophage (BMDM) were incubated with the lipid-coated targets. Cells were incubated with PC and PS- or PE-coated beads as well as 0.5% Cy5-PC to visualize the targets. After 10 min, the BMDM were incubated with LactC2-GFP or Dura-555 to distinguish between bound or internalized PS and PE beads respectively and imaged live. As shown in **Fig 2C** and

quantified in **Fig 2D**, both PS and PE coated beads were internalized by BMDM equally, suggesting that either lipid can serve as a phagocytic ligand.

To determine if apoptotic cells could also be detected and internalized by their exposure of PE, we first treated primary murine splenocytes with STS for 3-4 h. These targets were determined to be primarily apoptotic but did not become necrotic in this time frame, as determined by their impermeability to propidium iodide (not shown). As expected, once incubated with BMDM, these apoptotic splenocytes were readily bound and engulfed by the BMDM (**Fig 2E-F**). To then block externalized PS or PE, the apoptotic splenocytes were pre-incubated with LactC2 or Duramycin respectively. Remarkably, we found that blocking either PS or PE prevented engagement of targets by BMDM (**Fig 2E-F**). It is unclear how both LactC2 and Duramycin block particle capture by the macrophage, though this could relate to *i*) cooperativity of the two ligands and their respective receptors or *ii*) the obstruction of both ligands by the lipid binding agents.

Integrins and the Syk tyrosine kinase are required to initiate PE-mediated phagocytosis

Integrins are made active and participate in various types of phagocytosis, including efferocytosis (Albert *et al*, 2000; Hanayama *et al*, 2002; Savill *et al*, 1990). Once active, integrins connect extracellular ligands to the submembrane actin cytoskeleton via cytosolic bridging complexes that include talin, vinculin, and paxillin. The β2 integrins that are highly expressed on the surface of macrophages bind to a diverse array of target ligands, including lipids (Freeman & Grinstein, 2014). To determine if integrins may help to facilitate PE-mediated phagocytosis, similar to what had been shown for PS-mediated phagocytosis, we first fixed and immunostained BMDM for paxillin and vinculin shortly after their engagement of PE-containing

targets. Upon binding of PE-coated particles, BMDM showed clear recruitment of both integrin-associated proteins to the nascent phagocytic cup, indicating that integrins are likely active in the process (**Fig 3A**). Divalent cations are required for integrin activation. We therefore opted to remove divalent cations at the time of phagocytosis and chelated traces of these with EDTA to determine how this impacted the uptake of PE-containing targets. When BMDM were challenged with PE-targets in PBS/EDTA (Ca^{2+} and Mg^{2+} free), there was a 5-to-6-fold decrease in binding as compared to in D-PBS (which contains Ca^{2+} and Mg^{2+}) (**Fig 3B**). Taken together, integrins are likely mediators of PE-phagocytosis.

The activation of integrins requires their inside-out activation by signaling pathways downstream of other receptors. This often involves the phosphorylation and activation of adaptors and immunoreceptors which contain ITAMs. Phosphorylated ITAMs recruit kinases, notably the Syk tyrosine kinase, which feature in various types of phagocytosis (Jaumouille *et al*, 2019; Murakami *et al.*, 2014; Rosales & Uribe-Querol, 2017). Syk recruitment leads to the activation of its downstream effectors including PI3 kinases, GTPases including Rac, and phospholipase C, all of which support the activation of integrins (Mocsai *et al*, 2010). To determine if Syk activation was required for the phagocytosis of PE-containing targets, BMDM were pre-treated with a Syk inhibitor, BAY 61-3606, before challenging the cells with the PE-containing beads. After 10 min of incubation, the conjugates were labelled for external PE and the phagocytic efficiency was determined. Treatment of BMDM with the Syk inhibitor decreased the phagocytic efficiency of PE-targets from 80% to 20% (**Fig 3C-D**). These results would suggest that signaling from PE-receptors leads to Syk and integrin activation to trigger phagocytosis.

CD300a and CD300b bind PS and PE

Few receptors bind directly to PS or PE. Of these, TIM-1, TIM-3, TIM-4 and BAI1 are examples, though their surface expression level in unstimulated macrophages is restricted (Freeman *et al*, 2010; Naeini *et al*, 2020). Work on the CD300 family of receptors has identified PS and PE as being directly engaged by CD300a (an inhibitor receptor) and CD300b (a receptor that associates with ITAM-containing adaptors) (Murakami *et al.*, 2014; Simhadri *et al.*, 2012). We found that CD300a and CD300b were well-expressed in BMDM, where CD300a expression was depressed upon stimulation of the cells with LPS while CD300b expression was increased (**Fig 3E**). To determine the relative contributions of CD300a and CD300b for PE-mediated phagocytosis, we opted to first express these individually in mouse embryonic fibroblasts (MEF), which are normally non-phagocytic. To this end, CD300a- or CD300b-OFP were ectopically expressed in the MEF cells which were then challenged with PE- or PS-containing targets for comparison. Interestingly, both CD300a and CD300b conferred on cells the ability to bind PE-containing targets to nearly an equal extent as PS-containing targets which was not observed for PC alone (**Fig 3F-G**).

CD300a- and CD300b-expressing MEF cells appeared to only bind, but not internalize targets **(Fig 3H)**. CD300b can associate with the ITAM-containing adaptors DAP10 and DAP12 to promote its signaling. We therefore reperformed these experiments by also expressing DAP12-GFP together with CD300b and imaged with Dura-Cy5 to detect beads not internalized. Here, we found that MEF cells now gained the ability to phagocytose PE beads (**Fig 3H**). The sealed phagosomes that formed in the MEF cells appeared to contain CD300b, further suggesting that the receptor is tightly-engaged to the PE-containing target particles.

The balance of CD300a and CD300b signaling dictates the phagocytosis of PE targets

Thus far, CD300b appeared to be an activating receptor that triggers downstream signaling via ITAM-adaptors and integrins to allow for the uptake of PE targets. To investigate if CD300b is required for the phagocytosis of PE targets, the receptor was blocked using a monoclonal antibody. This was done 5 min before challenging BMDM with PE-containing targets for 10 min in serum free media as done previously. Targets were again imaged with Dura-555 to detect those not internalized. When compared to an isotype control antibody, blocking CD300b indeed caused the phagocytic efficiency of PE targets to decrease from 55% to 35% (**Fig 3**). CD300b is clearly not the only receptor involved in PE-target uptake: other receptors, including TIM-4, may be involved (Feng *et al*, 2010; Flannagan *et al*, 2014).

RAW264.7 cells are a good model for Fc- and complement-mediated phagocytosis as these cells express the appropriate receptors for these functions. We have found that this cell line is comparatively quite poor at achieving efferocytosis (see **Fig 3L-M** for example) and, interestingly, expresses high levels of CD300a (**Fig 3J**). To investigate a putatively inhibitory role for CD300a in PE-particle uptake in RAW264.7 cells, we edited the gene using CRISPR. Knockouts were validated using live labelling with an anti-CD300a antibody and quantitative PCR (**Fig 3J-K**). We then challenged the WT and KO cells with PE-containing targets, using PS-targets as a comparison. Cells were imaged using LactC2-GFP or Dura-Cy5 which were incubated without permeabilization to mark targets that were bound but not phagocytosed. When compared to unedited (WT) RAW264.7 cells, the CD300a KO cells had a 3- to 5-fold enhanced ability to internalize both PS and PE beads (**Fig 3L-M**). These data would suggest that CD300a is an inhibitory receptor that can repress PE-mediated phagocytosis.

Bacterial vesicles expose PE and are bound by macrophages

Cell death is accompanied by the exposure of both PS and PE and there are many bridging molecules that engage PS and facilitate rapid efferocytosis (Naeini *et al.*, 2020). Why then do myeloid cells express receptors that also engage PE? It may be that similarities between the phospholipid headgroups have resulted in receptors that manage to recognize both lipids serendipitously. However, there are several phagocytic targets that are likely to contain PE and not PS. Organelles, including mitochondria for example, do not contain PS but have an abundance of PE (Daum & Vance, 1997) and if released by necrotic cells would need to be contained by phagocytosis. Bacteria also contain little to no PS in their cell membranes while having a high concentration of PE (Sohlenkamp & Geiger, 2016). While bacteria are enclosed in cell walls that mask membrane lipids, their shedding of extracellular vesicles (EVs) (Toyofuku *et al.*, 2023) or the removal of the cell wall by extracellular lysozyme would expose PE, scrambled in the denuded membrane, to receptors.

We therefore endeavored to first investigate the membrane topology of bacteria upon scrambling their outer membrane bilayer with polymyxin. Specifically, GFP-expressing *E coli* were treated with lysozyme and polymyxin B, which lead to the expected formation of spheroplasts (**Fig 4A**) (Renner & Weibel, 2011). Convincingly, the spheroplasts exposed PE, as detected with Dura-555 which was only very rarely exposed in control bacteria, curiously seen at the septum that forms during cell division (**Fig 4A**). On challenging BMDM with the spheroplasts, we found that binding was decreased when PE was blocked with the duramycin (**Fig 4B-C**). The duramycin did not entirely block particle binding, indicating the presence of other phagocytic ligands on the spheroplasts in addition to PE. Bacteria also produce extracellular vesicles: we found that the supernatant fractions of growing bacteria contained EVs

as detected by electron microscopy (**Fig 4D**) and intimated by lipid detection using the FM-4-64 dye (**Fig 4E**). Interestingly, a majority of the FM-4-64 labeled EVs did not react with succinimidyl esters, suggesting low protein abundance in the vesicles (not shown). Using Dura-555, we found that the vesicles were, however, high in PE (**Fig 4E-F**). We found that the incubation of the bacterial EVs with BMDM resulted in their robust binding and internalized in a manner that seemed to largely depend on PE since blocking the lipid headgroup with duramycin prevented their uptake (**Fig 4G-H**).

To examine the mechanism of binding further, we generated liposomes of <1 μm in diameter that contained 5% PE and 0.5% Cy5-PC which provided a sufficient quantum yield to detect individual particles; this was not possible for the bacterial EVs which were only well-detected when they became concentrated in endolysosomes. The liposomes were subsequently incubated with fibroblasts expressing CD300a, which binds to PE but does not instigate internalization. As clearly shown in **Fig 4I**, we found that CD300a conferred on the fibroblasts the ability to bind to the PE-containing liposomes. This would suggest that small lipid particles can be engaged by CD300a, as was observed for larger PE-coated targets.

Discussion

The collapse of lipid bilayer asymmetry upon cell death is highly conserved. The process is facilitated by the activation of scramblases and the inactivation of energy-supported flippases and floppases. Lipid scrambling is in fact essential for the vesiculation (blebbing) that accompanies apoptosis (Ousingsawat *et al*, 2015) and membrane repair (Wu *et al.*, 2020); we also noted that activation of the TMEM16F scramblase alone was sufficient to cause membrane blebbing. The outer leaflets of membrane vesicles and debris that are shed from cells thus

become rich in lipids normally restricted to the inner leaflet. These same structures tend to exclude the bulky glycocalyx (Le *et al*, 2024) enabling the exposure of scrambled lipid head groups to phagocytic receptors.

Most studies have focused on the engagement of PS, either directly or indirectly, since there are select receptors that bind to this lipid and many others that bind to PS-associated bridging molecules like MFG-E8, Gas6, and Protein S (Arandjelovic & Ravichandran, 2015; Lemke, 2019). These bridging molecules are engaged by receptor tyrosine kinases of the MERTK family, which rapidly signal for the phagocytosis of the particle (Lemke & Rothlin, 2008). Curiously, MFG-E8, Gas6, and Protein S are all synthesized and released in specific tissues and, in some cases, with a circadian rhythm that supports regular phagocytic programs by resident phagocytes (Parinot *et al*, 2024). In certain contexts, bridging molecules may be limiting. However, the direct recognition of PS by TIM-1, -3, and -4 is another important mechanism for initiating the phagocytosis of dead cells (Wu *et al*, 2006) which would stand to achieve removal in these cases. There are clearly many inputs and receptors that facilitate the phagocytosis of apoptotic cells and debris which amounts to enough redundancy that other receptor-ligand pairs would not need to be evoked.

Yet, in this report, we find that PE can also serve as phagocytic ligand that leads to phagocytosis that proceeds as efficiently as that supported by the recognition of PS in the absence of serum. While the inner leaflet of the plasma membrane is richly endowed with PS, PE is just as prevalent. Endomembranes, notably the mitochondrial membrane, contain little PS and have high amounts of PE (Horvath & Daum, 2013). Chylomicrons may also be much higher in PE compared to PS and PE has been proposed to support removal of lipoproteins from circulation (van der Veen *et al*, 2017). Additionally, prokaryotic cells, which can shed vesicles

devoid of a glycocalyx/cell wall, contain little PS in their membranes (Bogdanov *et al.*, 2020). Clearly there are biologically important scenarios where PS is not present to signal the removal of dangerous particulates. In these settings, the recognition of PE may be a critical determinant for phagocytosis. The CD300 family, including CD300a and CD300b, are likely to feature in such situations (Cannon *et al.*, 2012; Murakami *et al.*, 2014; Nakahashi-Oda *et al.*, 2012; Simhadri *et al.*, 2012).

We found that CD300b is upregulated in inflammatory conditions while CD300a is downregulated. The relative expression of these family members across cell types could compartmentalize immune responses. While CD300a does not initiate phagocytosis, it could tether particulates to the plasma membrane and remove these through ongoing membrane turnover, i.e. by macropinocytosis. The inhibitory signaling from CD300a could also be anti-inflammatory (Tanaka *et al*, 2014; Zenarruzabeitia *et al*, 2015) and may turn off lytic responses of killer cells when they encounter the dead (Vitalle *et al*, 2019). CD300b, on the other hand, is likely more highly expressed on professional phagocytes, and stands to be a receptor that facilitates the uptake and destruction of PE- and PS-containing particles.

The recognition and removal of bacterial EVs and debris at mucosa is an interesting line of inquiry. For example, it is not yet understood how vesicles produced by the microbiome in the gut, skin, etc. affect immune tolerance or even if these vesicles are bound by resident phagocytes in these tissues. The specific set of receptors that are deployed at this interface therefore remains critical to determine. Moreover, the interactions between microbial species and the use of EVs to impact populations at a distance is also intriguing. Are these vesicles fusogenic and, if so, what mediates the delivery of their payloads between microbes? Curiously, duramycin is an antimicrobial peptide produced by *Streptomyces* (Fredenhagen *et al*, 1990). *Streptomyces* protect

their own PE from the peptide by its methylation (Huo *et al*, 2017). It is not yet understood precisely how duramycin exerts its effects, but the neutralization of bacterial EVs seems like a possible mode of action. More broadly, the receptors and functions of exofacial PE, whether in eukaryotic or prokaryotic membranes, is important for the field to consider going forward.

Methods

Cell culture

RAW264.7 and MEF cells were acquired from the American Type Culture Collection. Cells were cultured in DMEM (Wisent Cat# 319-007-CL) containing 5% FBS (Corning Cat#35-077-CV) and incubated at 37ºC with 5% CO_2. MEF cells were lifted using 0.25% trypsin (Wisent Cat# 325-043-CL). Bone marrow from the long bones from 8–12-week-old C57Bl/6 mice was washed with DMEM with serum and antibiotics then centrifuged. The pellet was resuspended into petri dishes containing 10% L929 fibroblast conditioned DMEM with 10% FBS, penicillin G, streptomycin, and amphotericin B (Wisent Cat# 450-115-EL). Cells were incubated at 37ºC for 4-6 days. Bone marrow-derived macrophages (BMDMs) were lifted using PBS and 5 mM EDTA, scraped and seeded on coverslips or culture dishes for 24-48 h. Splenocytes were isolated from 8–12-week-old C57Bl/6 mice. The spleen was removed from animals sacrificed by cervical dislocation. The spleen was homogenized by using the flat end of a syringe plunger through a 40 µm cell strainer, collected in a 50 mL centrifuge tube with PBS. Splenocytes were centrifuged at 400 g for 5 min then treated with cold RBC lysis buffer for 5 min. After centrifugation at 400 g for 5 min cells were resuspended in RPMI 1640 medium (Wisent Cat#350-00-CL) with 10% FBS and plated in 6 well plates.

For transient transfections, cells were seeded on glass coverslips within a 12 well plate the day prior. In a 1.5 mL tube, 50 µL serum-free DMEM and 1 µg of plasmid DNA was incubated for 5 min. 3 µL of FuGeneHD (Promega Cat# E2311) was added and incubated for an additional 15 min, then added to the seeded cells. Media was changed 4 h after transfection and cells were imaged the following day. MEF cells were transfected with the following plasmids: CD300a-OFPSpark (Sino Biological Cat# MG50675-ACR), CD300b-OFPSpark (Sino Biological Cat#CG90264-ACG) or CD300b-OFPSpark and DAP12-GFP (Sino Biological Cat#MG53479-ACG).

To generate knockout cells, parental RAW264.7 cells were plated in a 6 well plate. The following day these cells were transfected with a Guaranteed Predesigned CRISPR gRNA plasmid against CD300a (Sigma-Aldrich Cat#MMPD0000125274) or TMEM16F (Sigma-Aldrich Cat#MMPD0000108662). Cells were transfected with 500 µg of DNA and 1.5 µL of FugeneHD per well. Single, live (PI-negative), GFP-positive cells were sorted using FACS into 96 well tissue culture plates. CD300a knockouts were validated using live imaging and qPCR.

Sleeping Beauty TMEM16F knock-in assay

To test the activity of Ca^{2+} activated scramblase TMEM16F, HeLa cells with doxycycline inducible expression of WT or active mutant Y563Q TMEM16F generated in lab were used. Cells were treated with doxycycline hyclate (Sigma-Aldrich Cat#D9891) for 24 h prior to imaging. Cells were imaged using AnV-647 (AAT Bioquest Cat20074) and Dura-555.

Generation of lipid targets

Lipid targets were generated according to protocol by Joffe et. al(Joffe *et al*, 2020). Briefly, 4.98 µm silica beads were washed using piranha solution. Small unilamellar vesicles (SUVs) were generated by combining PC (Avanti Polar Lipids Cat#850457C25MG), PC-Cy5 (Millipore Sigma, Cat#850483C), PS (Millipore Sigma Cat# 840035C), or PE (Millipore Sigma Cat#850725C) according to Table 1. To generate targets, 160 µL MOPS buffer, 40 µL SUVs and 20 µL clean beads were incubated for 30 min, centrifuged and gently resuspended in 400 µL of PBS.

Vesicle type	Composition
PC only	100% PC
PS only	95% PC, 5% PS
PE only	95% PC, 5% PE
Fluorescent PC	99.6% PC, 0.4% PC-Cy5
Fluorescent PS	94.6% PC, 0.4% PC-Cy5, 5% PS
Fluorescent PE	94.6% PC, 0.4% PC-Cy5, 5% PE

Table 1. SUV composition

Lipid-binding probes

To detect PS, recombinant LactC2-GFP was generated in lab according to protocol by Yeung et al(Yeung *et al*, 2008). To detect PE, Duramycin-Cy5 (Molecular Targeting Technologies Cat#D-1002) or Duramycin-555 was generated in lab. Duramycin (Santa Cruz Cat#1391-36-2) and iFluor® 555 succinimidyl ester (Cedarlane Cat#1023) were added to 0.05 M borate buffer, vortexed, and incubated shaking at 500 rpm for 1 h at room temperature.

Duramycin-555 was dialyzed in 1 L PBS to remove unincorporated dye using 2000 Da Slide-A-Lyzer™ Dialysis Cassettes (Thermo Fisher Cat#66205). Collected Duramycin-555 was diluted 1:5 in PBS and stored in the freezer. To validate probes, PS- or PE- targets were incubated with both LactC2-GFP and Dura-555 and imaged. LactC2-GFP was used at 1:50, Dura-Cy5 at 1:50, and Dura-555 at 1:100. Samples with Dura-Cy5 were washed 1x with PBS before imaging.

Quantitative RT-PCR

RAW264.7 cells were plated in 6-well plates. After 24 h, cells were scraped, and RNA was extracted using E.Z.N.A. HP Total RNA Isolation Kit (VWR CA101414-852). 1 µg RNA from each condition was used to generate cDNA with qScript cDNA SuperMix (VWR Cat#101414-104) according to manufacturing protocols. Into each well in a 96-well plate, 2 µL of cDNA, 5 µL of TaqMan Fast Advanced Master Mix (Thermo Scientific Cat#4444556), 2 µL of water, 0.5 µL of Taqman probe for CD300a (Thermo Scientific Cat#4448892) and 0.5 µL reference gene Abt1 probe (Thermo Scientific Cat#4448489) was added. RT-qPCR was performed using QuantStudio 3 RT-qPCR System (Applied Biosystems, Thermo Fisher Scientific). 3 biological replicates were used per condition. The ΔΔCt method was used to determine relative gene expression.

Immunofluorescence

For immunofluorescence staining, PE targets were added to BMDM, centrifuged and immediately fixed with 4% PFA (Electron Microscopy Sciences Cat#15710) for 10 min. Samples were permeabilized with 0.5% triton for 5 min then blocked for 1 h with 5% BSA in PBS. Primary antibodies against paxillin (BD Transduction Cat#612405) or vinculin (EMD Millipore

Cat#MAB3574), were diluted 1:250 in blocking buffer and added to coverslips overnight at 4ºC. Samples were washed 3 times with PBS. Secondary antibody donkey anti mouse-488 (Jackson ImmunoResearch Cat#715-545-150) and phalloidin-555 (Cytoskeleton Cat#PHDH1-A) was incubated with coverslips for 45 min and washed 3 times with PBS before imaging.

Cell death assays

RAW264.7 cells were incubated with 1 μM staurosporine (Sigma-Aldrich S5921) for 3 h or 5 μM ionomycin (Sigma-Aldrich Cat#407950) for 15 min prior to imaging. RAW264.7 TMEM16F KO cells were incubated with ionomycin for 15 min prior to imaging. Cells were imaged with LactC2-GFP and Dura-555.

Phagocytosis

For binding and internalization assays with PS and PE targets, RAW264.7 cells, BMDM or MEF cells were plated on glass coverslips into a 12-well plate. Cells were washed with serum free media prior to addition of PS or PE targets. PS or PE targets were mixed with 1 mL of serum free media and added to cells at approximately a 20:1 ratio. Targets were incubated with cells for 10 min and washed gently before imaging live. For experiments inhibiting Syk in BMDM, cells were treated with 1 μM BAY 61-3606 (Cayman Chemical Company Cat#11423) for 10 min prior to addition of targets. For binding assays, beads bound per cell was calculated from images acquired using 25x objective and at least 10 fields of view using the following equation, $\frac{Total\ beads\ bound}{Total\ number\ of\ cells} \times 100$. For internalization assays, cells were imaged with LactC2-GFP or Dura-555 to mark outside beads. Phagocytic efficiency was calculated from images acquired

using 25x objective, and at least 10 fields of view using the following equation

$$\frac{Total\ targets - Outside\ targets}{Total\ targets} \times 100.$$

For MEF cell binding assays, MEF cells were transfected with CD300a-OFP or CD300b-OFP. Cells were incubated with PC, PS or PE targets and imaged live. Binding of targets was quantified as described above. For MEF cell internalization assays, cells were transfected with CD300b-OFP and DAP12-GFP. Cells were incubated with PE-targets and imaged live with Dura-Cy5.

To assay for the involvement of integrins, BMDM were plated on glass coverslips in a 12-well plate. Coverslips were washed with and incubated in D-PBS (Wisent Cat#311-420-CL) or PBS/EDTA for 10 min with PE-targets. After incubation, cells were washed and imaged live.

Lipid blocking assay

To generate apoptotic splenocytes, cells were first labelled with CellTrace FarRed DDAO-SE (Invitrogen Cat#C34553) in PBS for 30 min. Cells were centrifuged at 400 g for 5 min and resuspended in PBS then treated with 1 μM staurosporine for 3 h. After treatment, apoptotic splenocytes were centrifuged and resuspended in PBS. To block PS or PE, apoptotic splenocytes were incubated with LactC2 or Duramycin for 2 min, centrifuged, and washed 3 times with PBS. BMDM were plated on glass coverslips in 12-well plates the day before. BMDM were labelled with CellTrace Blue (Thermo Scientific Cat#C34574), then washed with serum free media and incubated with apoptotic splenocytes in serum free media for 5 min. Cells were washed with PBS and fixed with 4% PFA. After fixation cells were imaged.

CD300b antibody blocking

To block CD300b, BMDMs were plated on coverslips in a 12-well plate the day before. Coverslips were transferred to a plate on ice and incubated with CD300b antibody (Bio-Techne Cat#MAB2580) diluted 1:50 in cold HBSS (Wisent Cat#311-515-CL) for 3 minutes. The coverslip was transferred to a well with serum free media and incubated with PE-targets for 10 minutes then imaged. To calculate number of splenocytes bound, splenocytes bound per cell was calculated from images acquired using 25x objective and at least 10 fields of view using the following equation, $\frac{Total\ splenocytes\ bound}{Total\ number\ of\ cells} \times 100$.

Live immunofluorescence staining

To label cells for CD300a, cells were seeding on coverslips in a 12-well plate the day before. Coverslips were transferred to a plate on ice and treated with 50 uL primary antibody against CD300a (Biolegend Cat#147901), diluted 1:50 in HBSS for 3 min. Cells were then incubated in secondary antibody diluted 1:100 in HBSS for 5 min. Coverslips were gently washed 3 times with HBSS and imaged.

Making spheroplasts and spheroplast phagocytosis

To prepare spheroplasts, 6 ml of overnight culture of GFP E.coli was centrifuged at 3100 g, 4°C for 10 min. After the supernatant was removed, the bacterial pellet was used for making spheroplasts based on the protocol of (Figueroa DM et al. J Vis Exp. 2018 Aug 11;(138):57904. doi: 10.3791/57904. PMID: 30148492; PMCID: PMC6126710.). The protocol is modified as follows: after the pellet was washed with 0.8 M sucrose, it was treated with a solution containing 150 µL of 1 M Tris-Cl (pH 7.8), 120 µL of 5 mg/mL lysozyme, and 151 µL of 0.125 M EDTA.

Finally, the spheroplasts were collected by centrifugation at 3100 g, 4 °C for 8 min. The supernatant was removed all but 100-150 µl of supernatant left to avoid disturbing the pellet.

The spheroplast pellet was then resuspended in 1 ml of Tyrode buffer (10 mM HEPES, 10 mM D-Glucose, 5 mM KCl, 140 mM NaCl, 1 mM $MgCl_2$, 2 mM $CaCl_2$). After that, the spheroplasts were treated with 200 µg/ml polymyxin for 13-15 min at room temperature. The suspension of spheroplasts was then divided into 2 equal portions. One portion was added with 1:1000 Dura-555, and incubated at room temperature for 3 min. After that, both samples (with and without Dura-555) were centrifuged at 3100 g, 4°C for 8 min. The pellets were then resuspended with 1 mL Tyrode buffer and added with 100 µg/ml FITC for 5-10 min at room temperature. The samples were then centrifuged at 3100 g, 4°C for 8 min. The pellets were washed with 1 mL Tyrode buffer. The centrifugation and washing steps were repeated three times. The spheroplasts were finally resuspended with 1 mL of serum-free DMEM. BMDMs were plated on coverslips in a 12-well plate the day before. 100 µl of each spheroplast sample was added to CellTrace Far Red DDAO-SE (Invitrogen; Cat# C34553) labeled BMDM. After spheroplasts were added to BMDM, the samples were centrifuged at 1000 rpm for 20 s, then incubated at 37°C, 5% CO_2 for 10 min. Phagocytosis was done in serum-free DMEM. After that, the samples were rigorously washed with PBS and then fixed with 4% PFA in PBS for 10 min at room temperature. After fixation, cells were imaged.

Extracellular vesicle isolation, liposomes, and bacterial debris binding assays

Bacterial extracellular vesicles were isolated as described previously (Meyer & Nodwell, 2024). *Escherichia coli* ATCC25922 and *Mycobacterium smegmatis* mc^2155 were grown in LB, *Staphylococcus aureus* ATCC29213 and *Acinetobacter baumannii* ATCC19606 were grown in

Muller Hinton II Broth, at 37°C with shaking at 220 rpm. Overnight cultures from single colonies were diluted; *E. coli* and *A. baumannii* 1:100 and grown for 4 h, *S. aureus* 1:1000 and *M. smegmatis* diluted 1:20 and grown for 24 h. Supernatants from bacteria were centrifuged to pellet cells at 3000xg for 10 min, the supernatant was filtered through 0.2µm PES filters, and then concentrated 40x using 10 kDa Amicon Ultra centrifugal filter units (Millipore Cat#UFC901024). Extracellular vesicles were isolated from this concentrated supernatant taking the first 3 mL of elution with PBS after a 4.5 mL void volume of qEV1 35 nm columns (Izon Science Cat.#IC1-35). Transmission electron microscopy images of *E. coli* vesicles negative stained with 2% uranyl acetate were taken on a Talos L120C (TEM imaging & analysis v5.0 SP4). To quantify PE in vesicles, *E. coli* vesicles were incubated with polylysine coated coverslips for 10 min, duramycin-Cy5 added and coverslips washed, then FM 4-64 added at 5 µg/mL. To assess PE content between species, vesicle protein concentration was measured by BCA assay (after 30 min incubation with 1% Triton X-100), and vesicles amounting to 500 ng of protein stained with 100 µM Duramycin-555 for 5 min. Excess stain was then removed by washing 100-fold with PBS using 100 kDa centrifugal filters (Millipore Cat#UFCF10024) at 3000xg. Fluorescence of vesicles and PE liposomes stained in the same manner was read in 96-well plates, excitation 500 nm emission 580 nm (Syngery H1, Biotek).

Similarly, to test vesicle binding to macrophages, EVs were stained with FM1-43, the sample was split and half was blocked with Duramycin, then washed with 100 kDa centrifugal filters, and incubated with macrophages for 15 min in serum free media. Cells were imaged live.

Imaging

Images were acquired using a Zeiss Axiovert 200M microscope with a 63x/1.4 NA oil objective or 25x/0.8 NA water objective operated by Volocity software (Perkin-Elmer). Images acquired were analyzed and quantified using Volocity and Fiji (NIH) software.

Statistical analysis

Data are presented as mean ± SEM. Statistical analysis was performed with GraphPad Prism 8. Statistical significance of data was determined using unpaired Student's *t* tests with $P < 0.05$ considered significant.

Acknowledgments

S.A.F is the recipient of a Canada Research Chair and was supported by PJT-181078 from the Canadian Institutes of Health Research (CIHR) and a Discovery Grant RGPIN-2022-04485 from the Natural Sciences and Engineering Research Council of Canada (NSERC).

References

Albert ML, Kim JI, Birge RB (2000) alphavbeta5 integrin recruits the CrkII-Dock180-rac1 complex for phagocytosis of apoptotic cells. *Nat Cell Biol* 2: 899-905
Arandjelovic S, Ravichandran KS (2015) Phagocytosis of apoptotic cells in homeostasis. *Nat Immunol* 16: 907-917
Bogdanov M, Pyrshev K, Yesylevskyy S, Ryabichko S, Boiko V, Ivanchenko P, Kiyamova R, Guan Z, Ramseyer C, Dowhan W (2020) Phospholipid distribution in the cytoplasmic membrane of Gram-negative bacteria is highly asymmetric, dynamic, and cell shape-dependent. *Sci Adv* 6: eaaz6333
Bretscher MS (1972) Asymmetrical lipid bilayer structure for biological membranes. *Nat New Biol* 236: 11-12

Briaud P, Carroll RK (2020) Extracellular Vesicle Biogenesis and Functions in Gram-Positive Bacteria. *Infect Immun* 88
Brown L, Wolf JM, Prados-Rosales R, Casadevall A (2015) Through the wall: extracellular vesicles in Gram-positive bacteria, mycobacteria and fungi. *Nat Rev Microbiol* 13: 620-630
Cannon JP, O'Driscoll M, Litman GW (2012) Specific lipid recognition is a general feature of CD300 and TREM molecules. *Immunogenetics* 64: 39-47
Daum G, Vance JE (1997) Import of lipids into mitochondria. *Prog Lipid Res* 36: 103-130
Doktorova M, Symons JL, Levental I (2020) Structural and functional consequences of reversible lipid asymmetry in living membranes. *Nat Chem Biol* 16: 1321-1330
Doran AC, Yurdagul A, Jr., Tabas I (2020) Efferocytosis in health and disease. *Nat Rev Immunol* 20: 254-267
Emoto K, Kobayashi T, Yamaji A, Aizawa H, Yahara I, Inoue K, Umeda M (1996) Redistribution of phosphatidylethanolamine at the cleavage furrow of dividing cells during cytokinesis. *Proc Natl Acad Sci U S A* 93: 12867-12872
Emoto K, Toyama-Sorimachi N, Karasuyama H, Inoue K, Umeda M (1997) Exposure of phosphatidylethanolamine on the surface of apoptotic cells. *Exp Cell Res* 232: 430-434
Feng D, Zhao WL, Ye YY, Bai XC, Liu RQ, Chang LF, Zhou Q, Sui SF (2010) Cellular internalization of exosomes occurs through phagocytosis. *Traffic* 11: 675-687
Flannagan RS, Canton J, Furuya W, Glogauer M, Grinstein S (2014) The phosphatidylserine receptor TIM4 utilizes integrins as coreceptors to effect phagocytosis. *Mol Biol Cell* 25: 1511-1522
Fredenhagen A, Fendrich G, Marki F, Marki W, Gruner J, Raschdorf F, Peter HH (1990) Duramycins B and C, two new lanthionine containing antibiotics as inhibitors of phospholipase A2. Structural revision of duramycin and cinnamycin. *J Antibiot (Tokyo)* 43: 1403-1412
Freeman GJ, Casasnovas JM, Umetsu DT, DeKruyff RH (2010) TIM genes: a family of cell surface phosphatidylserine receptors that regulate innate and adaptive immunity. *Immunol Rev* 235: 172-189
Freeman SA, Grinstein S (2014) Phagocytosis: receptors, signal integration, and the cytoskeleton. *Immunol Rev* 262: 193-215
Han TW, Ye W, Bethel NP, Zubia M, Kim A, Li KH, Burlingame AL, Grabe M, Jan YN, Jan LY (2019) Chemically induced vesiculation as a platform for studying TMEM16F activity. *Proc Natl Acad Sci U S A* 116: 1309-1318
Hanayama R, Tanaka M, Miwa K, Shinohara A, Iwamatsu A, Nagata S (2002) Identification of a factor that links apoptotic cells to phagocytes. *Nature* 417: 182-187
Horvath SE, Daum G (2013) Lipids of mitochondria. *Prog Lipid Res* 52: 590-614
Huo L, Okesli A, Zhao M, van der Donk WA (2017) Insights into the Biosynthesis of Duramycin. *Appl Environ Microbiol* 83
Irie A, Yamamoto K, Miki Y, Murakami M (2017) Phosphatidylethanolamine dynamics are required for osteoclast fusion. *Sci Rep* 7: 46715
Jaumouille V, Cartagena-Rivera AX, Waterman CM (2019) Coupling of beta2 integrins to actin by a mechanosensitive molecular clutch drives complement receptor-mediated phagocytosis. *Nat Cell Biol* 21: 1357-1369

Joffe AM, Bakalar MH, Fletcher DA (2020) Macrophage phagocytosis assay with reconstituted target particles. *Nat Protoc* 15: 2230-2246
Kay JG, Grinstein S (2011) Sensing phosphatidylserine in cellular membranes. *Sensors (Basel)* 11: 1744-1755
Le T, Ferling I, Qiu L, Nabaile C, Assuncao L, Roskelley CD, Grinstein S, Freeman SA (2024) Redistribution of the glycocalyx exposes phagocytic determinants on apoptotic cells. *Dev Cell*
Le T, Jia Z, Le SC, Zhang Y, Chen J, Yang H (2019) An inner activation gate controls TMEM16F phospholipid scrambling. *Nat Commun* 10: 1846
Lemke G (2019) How macrophages deal with death. *Nat Rev Immunol* 19: 539-549
Lemke G, Rothlin CV (2008) Immunobiology of the TAM receptors. *Nat Rev Immunol* 8: 327-336
Lorent JH, Levental KR, Ganesan L, Rivera-Longsworth G, Sezgin E, Doktorova M, Lyman E, Levental I (2020) Plasma membranes are asymmetric in lipid unsaturation, packing and protein shape. *Nat Chem Biol* 16: 644-652
Meyer KJ, Nodwell JR (2024) extracellular vesicles are a broad and permissive antimicrobial packaging and delivery system. *J Bacteriol* 206: e0032523
Mocsai A, Ruland J, Tybulewicz VL (2010) The SYK tyrosine kinase: a crucial player in diverse biological functions. *Nat Rev Immunol* 10: 387-402
Murakami Y, Tian L, Voss OH, Margulies DH, Krzewski K, Coligan JE (2014) CD300b regulates the phagocytosis of apoptotic cells via phosphatidylserine recognition. *Cell Death Differ* 21: 1746-1757
Naeini MB, Bianconi V, Pirro M, Sahebkar A (2020) The role of phosphatidylserine recognition receptors in multiple biological functions. *Cell Mol Biol Lett* 25: 23
Nakahashi-Oda C, Tahara-Hanaoka S, Honda S, Shibuya K, Shibuya A (2012) Identification of phosphatidylserine as a ligand for the CD300a immunoreceptor. *Biochem Biophys Res Commun* 417: 646-650
Ousingsawat J, Wanitchakool P, Kmit A, Romao AM, Jantarajit W, Schreiber R, Kunzelmann K (2015) Anoctamin 6 mediates effects essential for innate immunity downstream of P2X7 receptors in macrophages. *Nat Commun* 6: 6245
Parinot C, Chatagnon J, Rieu Q, Roux S, Neel D, Hamieh F, Nandrot EF (2024) Gas6 and Protein S Ligands Cooperate to Regulate MerTK Rhythmic Activity Required for Circadian Retinal Phagocytosis. *Int J Mol Sci* 25
Ragland SA, Criss AK (2017) From bacterial killing to immune modulation: Recent insights into the functions of lysozyme. *PLoS Pathog* 13: e1006512
Renner LD, Weibel DB (2011) Cardiolipin microdomains localize to negatively curved regions of Escherichia coli membranes. *Proc Natl Acad Sci U S A* 108: 6264-6269
Rosales C, Uribe-Querol E (2017) Phagocytosis: A Fundamental Process in Immunity. *Biomed Res Int* 2017: 9042851
Sakuragi T, Nagata S (2023) Regulation of phospholipid distribution in the lipid bilayer by flippases and scramblases. *Nat Rev Mol Cell Biol* 24: 576-596
Savill J, Dransfield I, Hogg N, Haslett C (1990) Vitronectin receptor-mediated phagocytosis of cells undergoing apoptosis. *Nature* 343: 170-173

Segawa K, Nagata S (2015) An Apoptotic 'Eat Me' Signal: Phosphatidylserine Exposure. *Trends Cell Biol* 25: 639-650
Simhadri VR, Andersen JF, Calvo E, Choi SC, Coligan JE, Borrego F (2012) Human CD300a binds to phosphatidylethanolamine and phosphatidylserine, and modulates the phagocytosis of dead cells. *Blood* 119: 2799-2809
Sohlenkamp C, Geiger O (2016) Bacterial membrane lipids: diversity in structures and pathways. *FEMS Microbiol Rev* 40: 133-159
Suzuki J, Denning DP, Imanishi E, Horvitz HR, Nagata S (2013) Xk-related protein 8 and CED-8 promote phosphatidylserine exposure in apoptotic cells. *Science* 341: 403-406
Suzuki J, Umeda M, Sims PJ, Nagata S (2010) Calcium-dependent phospholipid scrambling by TMEM16F. *Nature* 468: 834-838
Tanaka T, Tahara-Hanaoka S, Nabekura T, Ikeda K, Jiang S, Tsutsumi S, Inagaki T, Magoori K, Higurashi T, Takahashi H *et al* (2014) PPARbeta/delta activation of CD300a controls intestinal immunity. *Sci Rep* 4: 5412
Toyofuku M, Schild S, Kaparakis-Liaskos M, Eberl L (2023) Composition and functions of bacterial membrane vesicles. *Nat Rev Microbiol* 21: 415-430
van der Veen JN, Kennelly JP, Wan S, Vance JE, Vance DE, Jacobs RL (2017) The critical role of phosphatidylcholine and phosphatidylethanolamine metabolism in health and disease. *Biochim Biophys Acta Biomembr* 1859: 1558-1572
Verkleij AJ, Zwaal RF, Roelofsen B, Comfurius P, Kastelijn D, van Deenen LL (1973) The asymmetric distribution of phospholipids in the human red cell membrane. A combined study using phospholipases and freeze-etch electron microscopy. *Biochim Biophys Acta* 323: 178-193
Vitalle J, Terren I, Orrantia A, Perez-Garay R, Vidal F, Iribarren JA, Rodriguez C, Lirola AML, Bernal E, Zenarruzabeitia O *et al* (2019) CD300a inhibits CD16-mediated NK cell effector functions in HIV-1-infected patients. *Cell Mol Immunol* 16: 940-942
Wu N, Cernysiov V, Davidson D, Song H, Tang J, Luo S, Lu Y, Qian J, Gyurova IE, Waggoner SN *et al* (2020) Critical Role of Lipid Scramblase TMEM16F in Phosphatidylserine Exposure and Repair of Plasma Membrane after Pore Formation. *Cell Rep* 30: 1129-1140 e1125
Wu Y, Tibrewal N, Birge RB (2006) Phosphatidylserine recognition by phagocytes: a view to a kill. *Trends Cell Biol* 16: 189-197
Yamanishi Y, Kitaura J, Izawa K, Kaitani A, Komeno Y, Nakamura M, Yamazaki S, Enomoto Y, Oki T, Akiba H *et al* (2010) TIM1 is an endogenous ligand for LMIR5/CD300b: LMIR5 deficiency ameliorates mouse kidney ischemia/reperfusion injury. *J Exp Med* 207: 1501-1511
Yeung T, Gilbert GE, Shi J, Silvius J, Kapus A, Grinstein S (2008) Membrane phosphatidylserine regulates surface charge and protein localization. *Science* 319: 210-213
Zenarruzabeitia O, Vitalle J, Eguizabal C, Simhadri VR, Borrego F (2015) The Biology and Disease Relevance of CD300a, an Inhibitory Receptor for Phosphatidylserine and Phosphatidylethanolamine. *J Immunol* 194: 5053-5060
Zhao M, Li Z, Bugenhagen S (2008) 99mTc-labeled duramycin as a novel phosphatidylethanolamine-binding molecular probe. *J Nucl Med* 49: 1345-1352

Figures

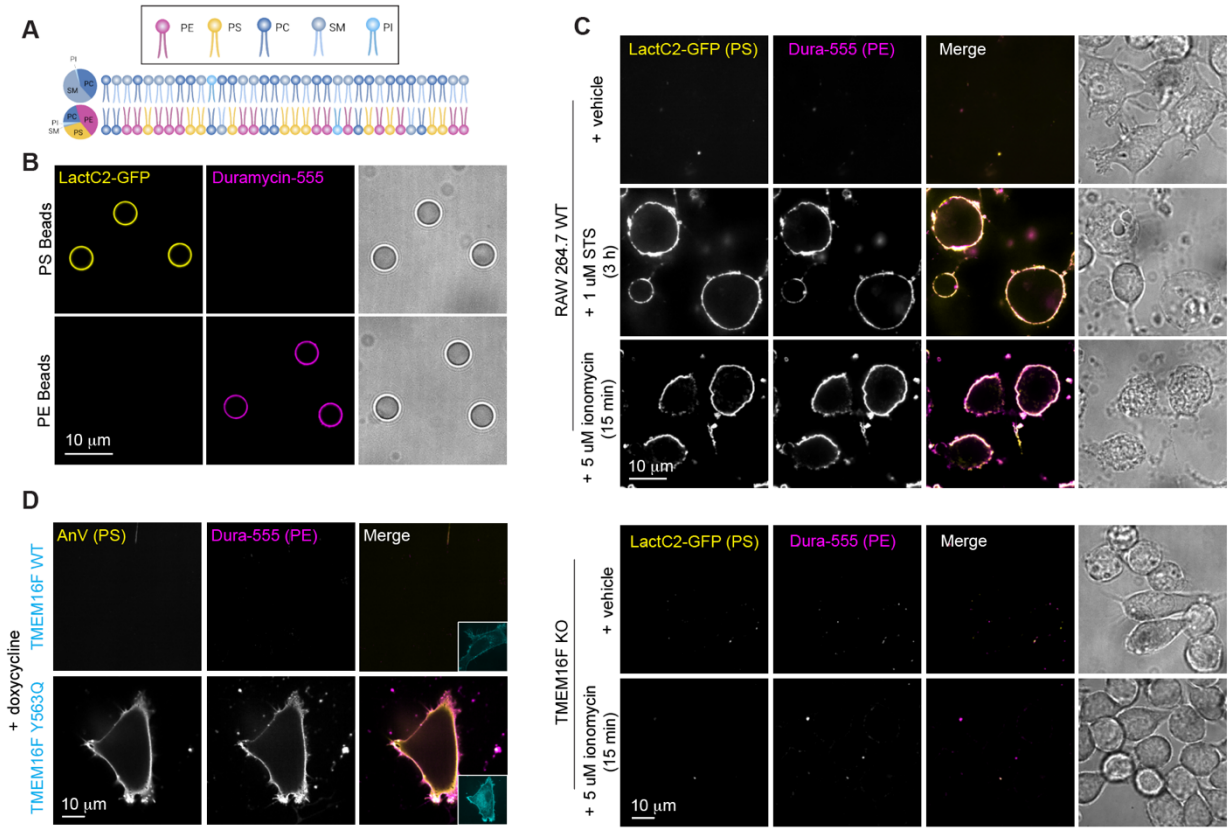

Figure 1. *PE is scrambled during cell death*. A) Model based on Doktorova et al., 2023. B) Labelling of lipid-coated beads containing 95% PC and 5% of either PS or PE as indicated with both LactC2-GFP and Dura-555 (n=3). C) WT RAW264.7 cells incubated with 1 µM STS or 5 µM ionomycin to activate lipid scrambling. Below, RAW264.7 TMEM16F KO cells incubated with 5 µM ionomycin. Cells imaged live with LactC2-GFP and Dura-555 (n=3). D) HeLa cells induced with doxycycline to express WT or a constitutively active form of TMEM16F (Y563Q). Cells imaged with AnnexinV and Dura-555. Scale bars, 10 µm.

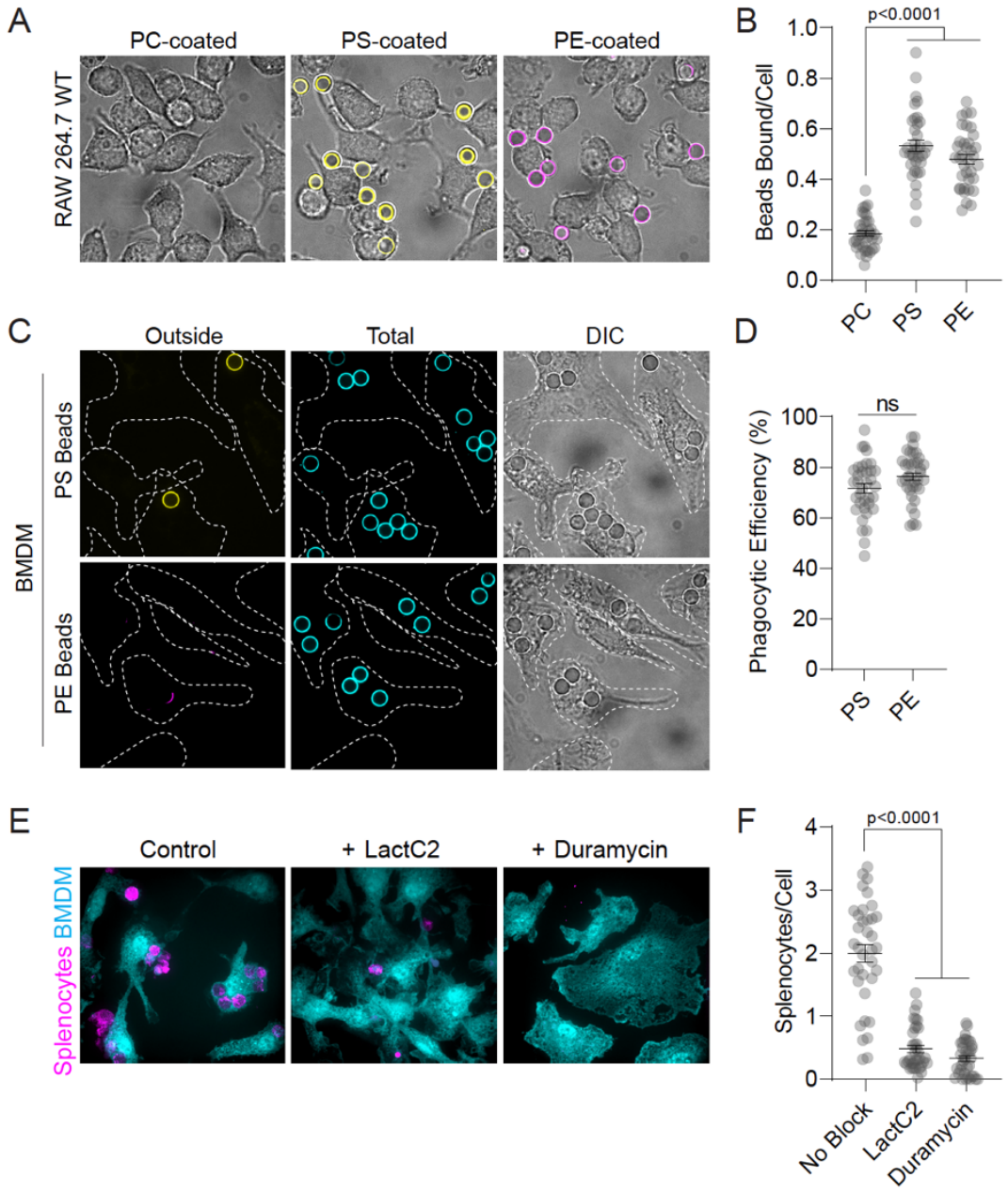

Figure 2. *PE is a phagocytic ligand*. A) Representative images and B) quantification of PC, PS and PE targets incubated with RAW264.7 cells. Total number of beads bound was divided by total number of cells in field of view (n=3). C) Representative images and D) quantification of PS and PE beads incubated with BMDM imaged live with LactC2-GFP and Duramycin-555 respectively. Phagocytic efficiency calculated by dividing inside beads by total beads (n=3). E) Representative images and F) quantification of CellTracker Blue labelled BMDM (cyan) incubated with CellTrace dyed apoptotic splenocytes (magenta) for 5 min. Apoptosis was induced by incubating splenocytes in 1 µM staurosporine for 3 h. Cells were fixed and imaged. Total number of splenocytes bound or internalized was divided by total number of cells in field (n=3). Scale bars, 10 µm. For B, D, F data are mean ± SEM, *p* values were calculated using Student's *t* tests.

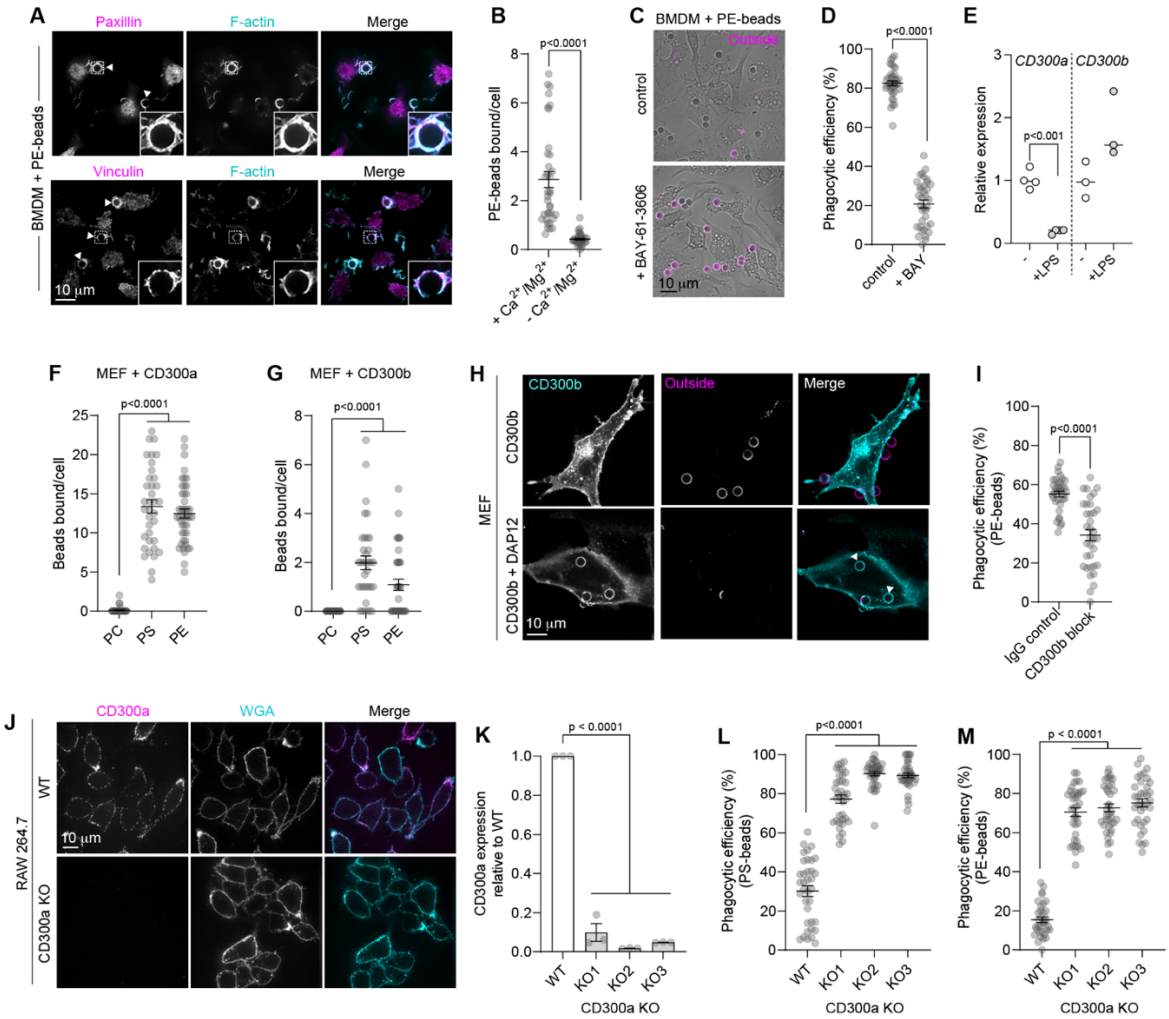

Figure 3. *Integrins, Syk, and CD300 receptors mediated PE phagocytosis.* A) F-actin (phalloidin), paxillin or vinculin in BMDM incubated with PS or PE beads for <1 min. Scale bar, 10 µm (n=3). B) Quantification of BMDM incubated in D-PBS (+ Ca^{2+}/Mg^{2+}) or PBS/EDTA (- Ca^{2+}/Mg^{2+}) with PE beads for 10 min. Beads bound/cell was calculated by dividing number of beads bound or internalized by total number of cells in field of view. C) Representative images and D) quantification of PE beads incubated for 10 min with untreated or 15 min, 1 µM BAY 61-3606 treated BMDM. Cells were imaged live with Dura-555. Percent internalized was calculated by dividing inside beads by total bead count. Scale bar, 10 µm. E) QPCR as indicated. F) Quantification of CD300a-OFP expressing and G) CD300b-OFP expressing MEF cells incubated with PS or PE beads in serum free DMEM for 10 min. H) Representative images of MEF cells transfected with CD300b-OFP alone or with DAP12-GFP and incubated with PE beads for 10 min. Cells were imaged live with Dura-Cy5 to label outside beads. Scale bar, 10 µm. I) Quantification of BMDM blocked with IgG or CD300b and incubated with PE beads for 10 min. Cells were imaged live with Dura-555. J) Surface staining of CD300a (magenta) and wheat germ agglutinin (WGA, cyan) of RAW 264.7 cells. Quantification of PS beads or J) PE beads incubated with WT or CD300a KO cells for 10 min and imaged with I) Lact-C2-GFP (n=3) or J) Duramycin-Cy5 (n=3). Phagocytic efficiency was calculated by dividing inside beads by total. Data are mean ± SEM, *p* value calculated using Student's *t* tests (n=3).

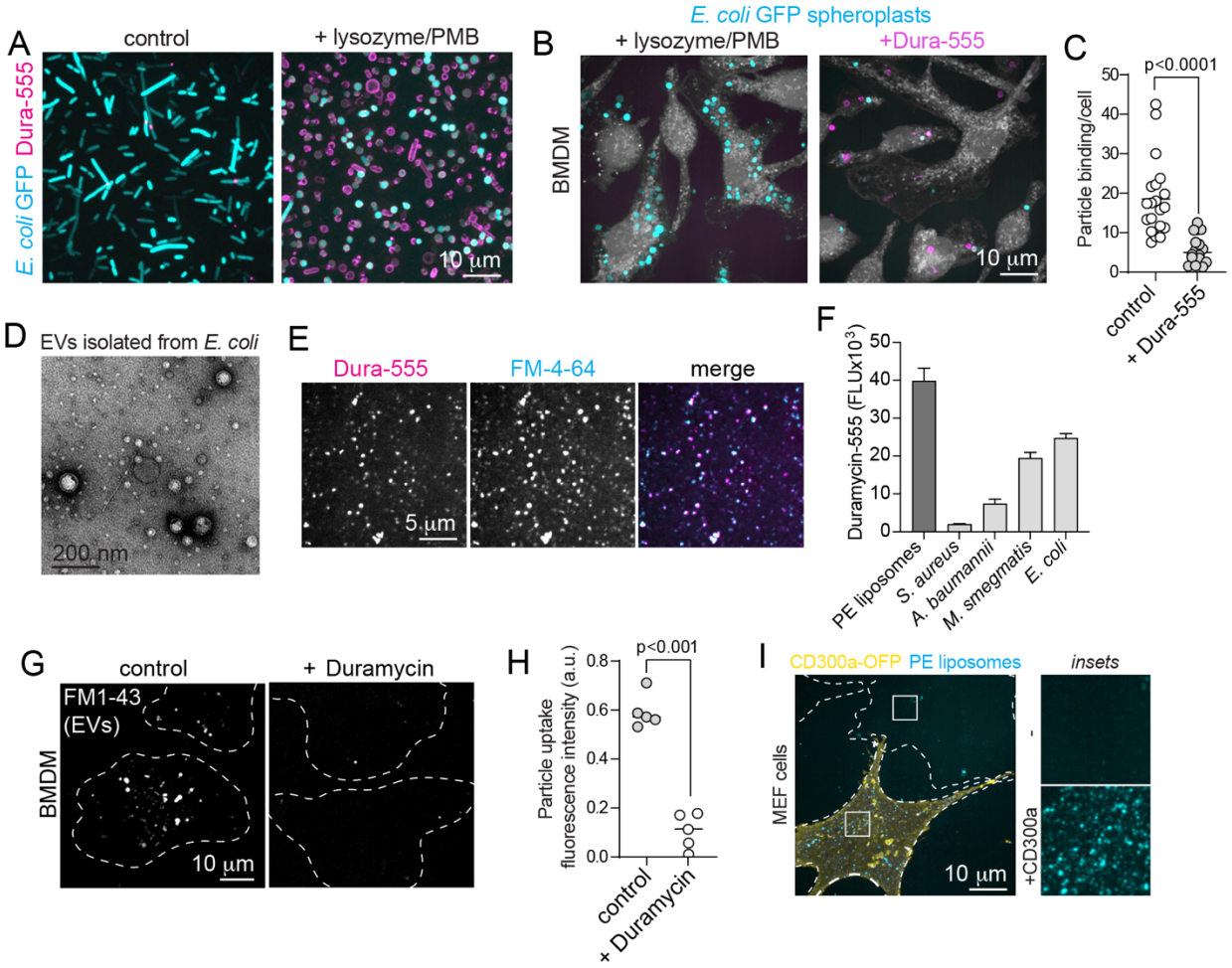

Figure 4. *PE engagement facilitates the binding of bacterial spheroplasts and vesicles.* A) Control GFP (cyan)-expressing *E. coli* or those incubated with lysozyme and polymyxin B (PMB) stained with Duramycin-555 (magenta). Scale bar, 10 µm (n=3). B-C) BMDM incubated with *E. coli* spheroplasts treated as in A, with or without pre-incubation with Duarmycin-555. Quantification of individual fields of BMDM each containing 5-10 cells. n=3. D) Representative TEM image of EVs isolated from E. coli. E) Representative image of *E. coli* EVs incubated with Duramycin-555 (magenta) and FM4-64 (cyan). F) Quantification of Duramycin-555 signal for various indicated particles determined by plate reader. The same number of particles were used in each case. G-H) BMDM incubated with FM1-43 labelled *E. coli* EVs for 20 min. I) Representative image of CD300a-OFP expressing MEF cells incubated with PE liposomes in serum free medium for 10 min.